Acta Cryst E CRYSTALLOGRAPHIC COMMUNICATIONS

ISSN 2056-9890

Zwitterionic 4-bromo-6-methoxy-2-{[tris(hydroxymethyl)methyl]iminiumylmethyl}phenolate: crystal structure and Hirshfeld surface analysis

See Mun Lee,* Kong Mun Lo, Sang Loon Tan and Edward R. T. Tiekink*

Research Centre for Crystalline Materials, Faculty of Science and Technology, Sunway University, 47500 Bandar Sunway, Selangor Darul Ehsan, Malaysia. *Correspondence e-mail: annielee@sunway.edu.my, edwardt@sunway.edu.my

Received 26 July 2016
Accepted 26 July 2016

Edited by W. T. A. Harrison, University of Aberdeen, Scotland

Keywords: crystal structure; zwitterion; hydrogen bonding; Hirshfeld surface analysis.

CCDC reference: 1496206

Supporting information: this article has supporting information at journals.iucr.org/e

In the solid state, the title compound, $C_{12}H_{16}BrNO_5$ [systematic name: 4-bromo-2-((1*E*)-{[1,3-dihydroxy-2-(hydroxymethyl)propan-2-yl]iminiumyl}methyl)-6-methoxybenzen-1-olate], $C_{12}H_{16}BrNO_5$, is found in the keto–amine tautomeric form, with an intramolecular iminium-N—H···O(phenolate) hydrogen bond and an *E* conformation about the C=N bond. Both *gauche* (two) and *anti* relationships are found for the methylhydroxy groups. In the crystal, a supramolecular layer in the *bc* plane is formed *via* hydroxy-O—H···O(hydroxy) and charge-assisted hydroxy-O—H···O(phenolate) hydrogen-bonding interactions; various C—H···O interactions provide additional cohesion to the layers, which stack along the *a* axis with no directional interactions between them. A Hirshfeld surface analysis confirms the lack of specific interactions in the inter-layer region.

1. Chemical context

Interest in molecules related to the title Schiff base compound derived from tris(hydroxymethyl)aminomethane (see Scheme) rests largely with the biological activity exhibited by their metal complexes. Thus, various species have been studied for their anticancer potential, *e.g.* vanadium (Back *et al.*, 2012) and tin (Lee *et al.*, 2015). The insulin-mimetic behaviour of vanadium complexes have been explored (Rehder *et al.*, 2002), as has the catecolase activity of binuclear cobalt complexes (Dey & Mukherjee, 2014). More recently, the adipogenic (cell differentiation) capacity of vanadium (Halevas *et al.*, 2015) and zinc complexes has been described (Tsave *et al.*, 2015). Over and above these considerations, magnetochemistry motivates on-going investigations, especially single-molecule (Wu *et al.*, 2007; Chandrasekhar *et al.*, 2013; Dey *et al.*, 2015) and lanthanide-containing species (Zou *et al.*, 2015; Das *et al.*, 2015). It was during on-going biological assays (Lee *et al.*, 2015) that the title compound, (I), became available. Herein, the crystal and molecular structures of (I) are described, as well as a Hirshfeld surface analysis.

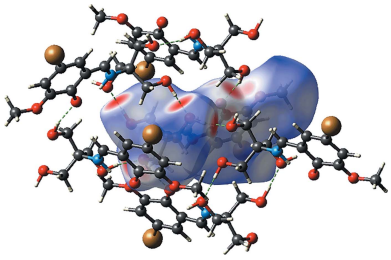

OPEN ACCESS

2. Structural commentary

The molecular structure of (I) (Fig. 1) exists as a zwitterion in the solid state, with the iminium N atom being protonated and the phenolate O atom being deprotonated. The observed keto–amine tautomeric form for (I) is the common form for molecules of this type, see *Database survey*. The conformation about the iminium bond [1.295 (4) Å] is *E* and this residue is almost coplanar with the benzene ring, forming a C2—C1—

C7—N1 torsion angle of 1.9 (4)°. This arrangement allows for the formation of a tight charge-assisted iminium-N—H···O(phenolate) hydrogen bond (Table 1). The conformations of the methylhydroxy groups are variable, with *gauche* relationships about the C8—C9 and C8—C11 bonds [N1—C8—C9—O2 is 45.9 (3)°, *i.e.* +synclinal, and N1—C8—C11—O4 is −80.2 (3)°, *i.e.* –synclinal], and an *anti* relationship about the C8—C10 bond [N1—C8—C10—O3 is 178.8 (2)°, *i.e.* +antiperiplanar]. The methoxy group is almost coplanar with the ring it is connected to, as seen in the value of the C12—O5—C3—C2 torsion angle of 177.7 (2)°.

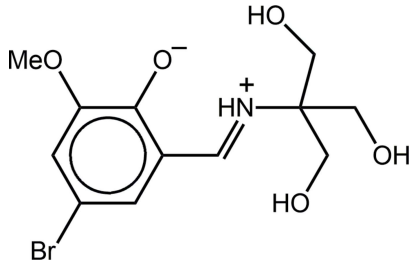

3. Supramolecular features

As anticipated from the chemical composition of (I), there are considerable hydrogen-bonding interactions operating in the crystal; geometric characteristics of these are listed in Table 1. Each of the hydroxy O2 and O3 atoms participates in hydroxy-O—H···O(hydroxy) hydrogen-bonding interactions, while the hydroxy O4 atom forms a donor interaction with the phenolate O1 atom. The result is the formation of a supramolecular layer parallel to (100) (Fig. 2*a*). Within this framework are a number of C—H···O interactions, *i.e.* imine-C7—H···O(phenolate), methylene-C11—H···O(phenolate) and methylene-C9—H···O(hydroxy) (Fig. 2*b*). In accord with the distance criteria in *PLATON* (Spek, 2009), layers stack along the *a* axis with no directional interactions between them. In order to gain more insight into the molecular packing of (I), a Hirshfeld surface analysis was conducted.

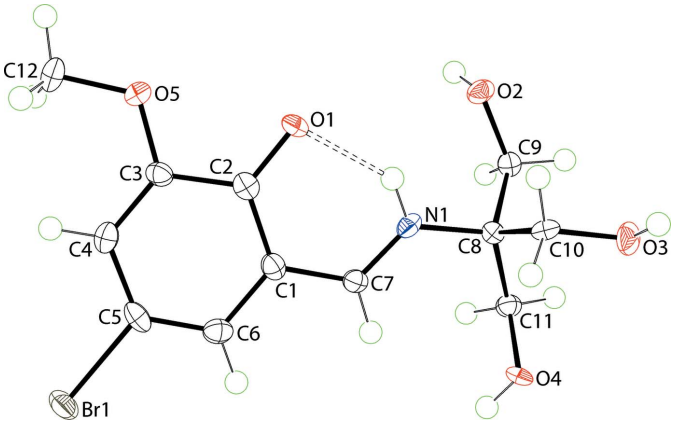

Figure 1
The molecular structure of (I), showing the atom-labelling scheme and displacement ellipsoids at the 70% probability level. The intramolecular N—H···O hydrogen bond is shown as a double-dashed line (see Table 1)

Table 1
Hydrogen-bond geometry (Å, °).

D—H···*A*	*D*—H	H···*A*	*D*···*A*	*D*—H···*A*
N1—H1N···O1	0.85 (2)	1.90 (2)	2.608 (3)	140 (3)
O2—H2O···O4^{i}	0.82 (2)	1.93 (2)	2.741 (3)	170 (3)
O3—H3O···O2^{ii}	0.81 (2)	1.91 (2)	2.704 (3)	167 (4)
O4—H4O···O1^{iii}	0.82 (3)	1.98 (3)	2.760 (3)	158 (3)
C7—H7···O1^{iii}	0.93	2.55	3.429 (4)	158
C9—H9*B*···O3^{i}	0.97	2.51	3.242 (4)	132
C11—H11*B*···O1^{iv}	0.97	2.39	3.353 (3)	171

Symmetry codes: (i) $-x+2, y-\frac{1}{2}, -z+\frac{3}{2}$; (ii) $-x+2, -y+1, -z+1$; (iii) $x, -y+\frac{1}{2}, z+\frac{1}{2}$; (iv) $-x+2, y+\frac{1}{2}, -z+\frac{3}{2}$.

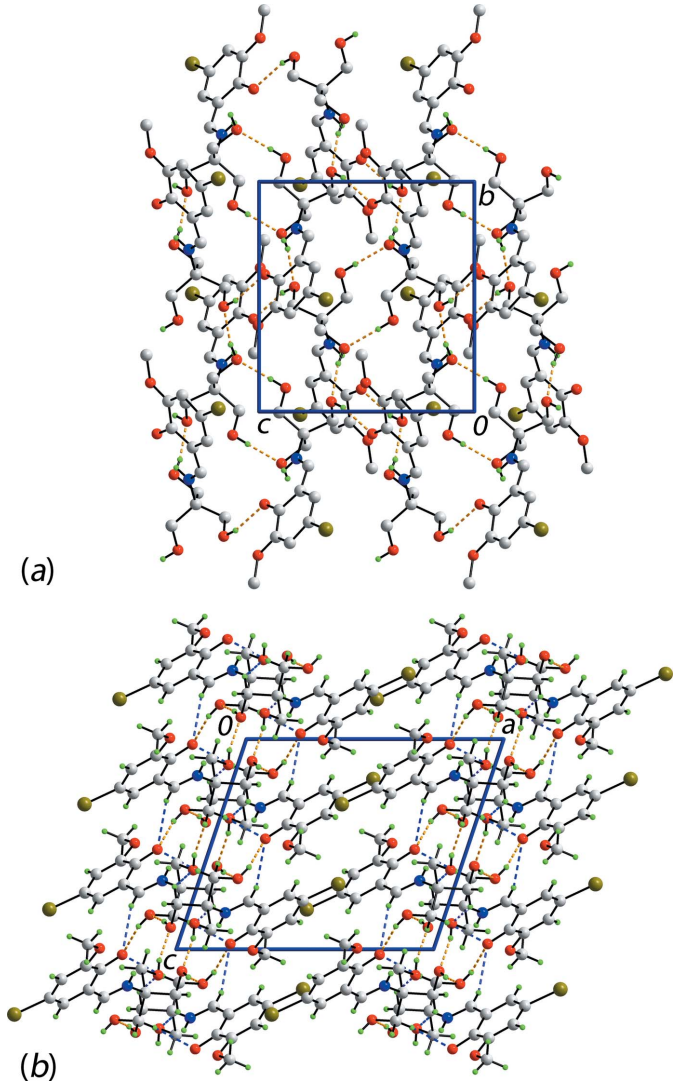

Figure 2
The molecular packing in (I), showing (*a*) a view of the supramolecular layer sustained by O—H···O hydrogen bonding, shown as orange dashed lines, and (*b*) a view of the unit-cell contents shown in projection down the *b* axis, highlighting the stacking of layers along the *a* axis. In (*a*), only acidic H atoms are shown.

4. Analysis of the Hirshfeld surfaces

The Hirshfeld surface of (I) was mapped over the d_{norm} contact distance within the range of −0.67 to 1.31 Å through calculation of the internal (d_i) and external (d_e) Hirshfeld surface distances to the nearest nucleus (McKinnon *et al.*, 2007; Spackman & Jayatilaka, 2009). Two-dimensional fingerprint plots associated with relevant close contacts were obtained through the plot of d_e *versus* d_i (Spackman & McKinnon, 2002). The electrostatic potential (ESP) of the crystal structure was mapped onto the Hirshfeld surface by an *ab initio* quantum modelling approach at the Hartree–Fock level of theory with the STO-3G basis set (HF/STO-3G) over the range of −0.122 to 0.189 au. All Hirshfeld surface and fingerprints plots were generated using *Crystal Explorer* (Wolff *et al.*, 2012), while the ESP was calculated by *TONTO* (Spackman *et al.*, 2008) as implemented in *Crystal Explorer*. Distances involving H atoms were normalized to the standard neutron diffraction bond lengths.

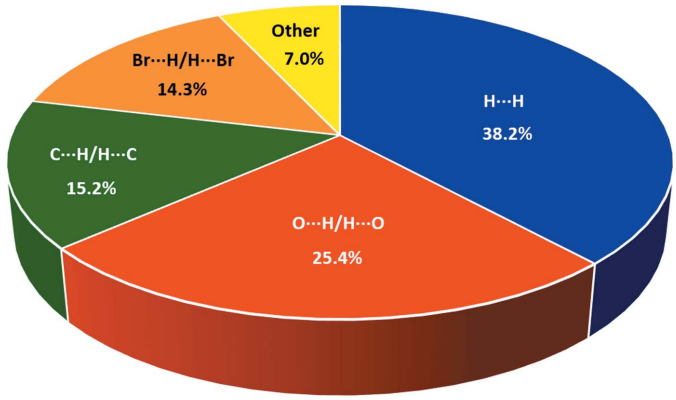

Figure 4
Percentage distribution of the corresponding close contacts to the Hirshfeld surface of (I).

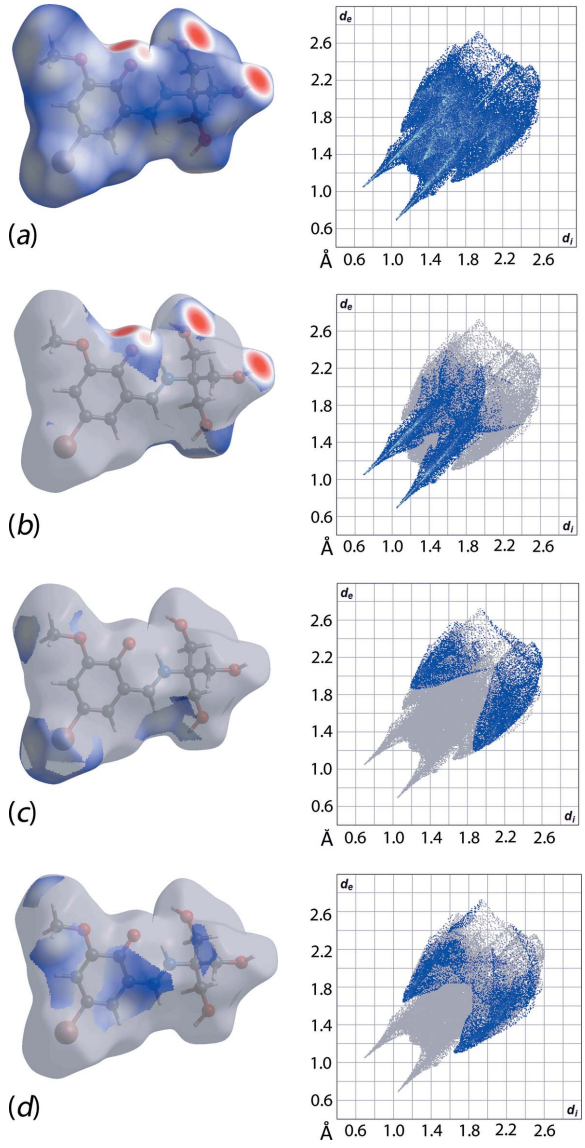

Figure 3
(*a*) Overall Hirshfeld surface and the two-dimensional fingerprint plot for (I), and d_{norm} surfaces and two-dimensional plots associated with (*b*) O···H/H···O, (*c*) Br···H/H···Br and (*d*) C···H/H···C interactions.

The Hirshfeld surface map provides a visual summary of any close contacts (shown as red) in contrast to relatively long contacts (shown as white and blue). As displayed in Fig. 3(*a*), there are several red spots observed on the Hirshfeld surface of (I), particularly around the O atoms, indicating close interactions at distances shorter than the sum of the van der Waals radii. A quantitative analysis of the decomposed two-dimensional fingerprint plot of the relevant O···H/H···O interactions reveals a distinctive reciprocal spike in the plot of d_e *versus* d_i (Fig. 3*b*), with the sum of contact distances being approximately 1.74 Å, signifying a strong intermolecular interaction. Such strong interactions constitute the second major contribution to the Hirshfeld surface, *i.e.* 25.4%, between the most prominent H···H (38.2%) and other major contacts, like C···H/H···C (15.2%) and Br···H/H···Br (14.3%) (Fig. 4). Their contributions to the overall Hirshfeld

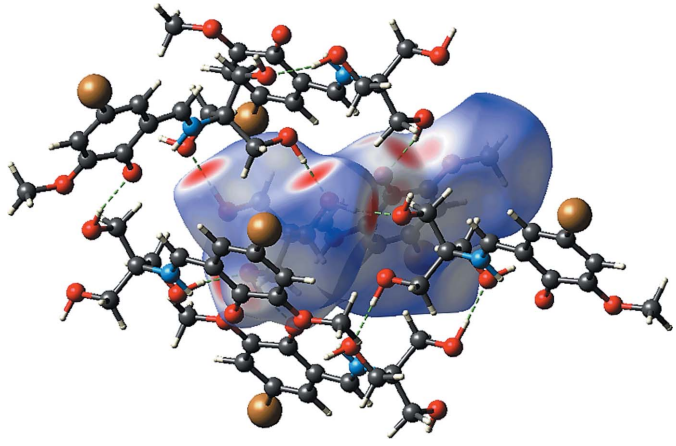

Figure 5
The d_{norm} surface for (I), highlighting the O···H hydrogen-bonding interactions which connect molecules in the molecular packing.

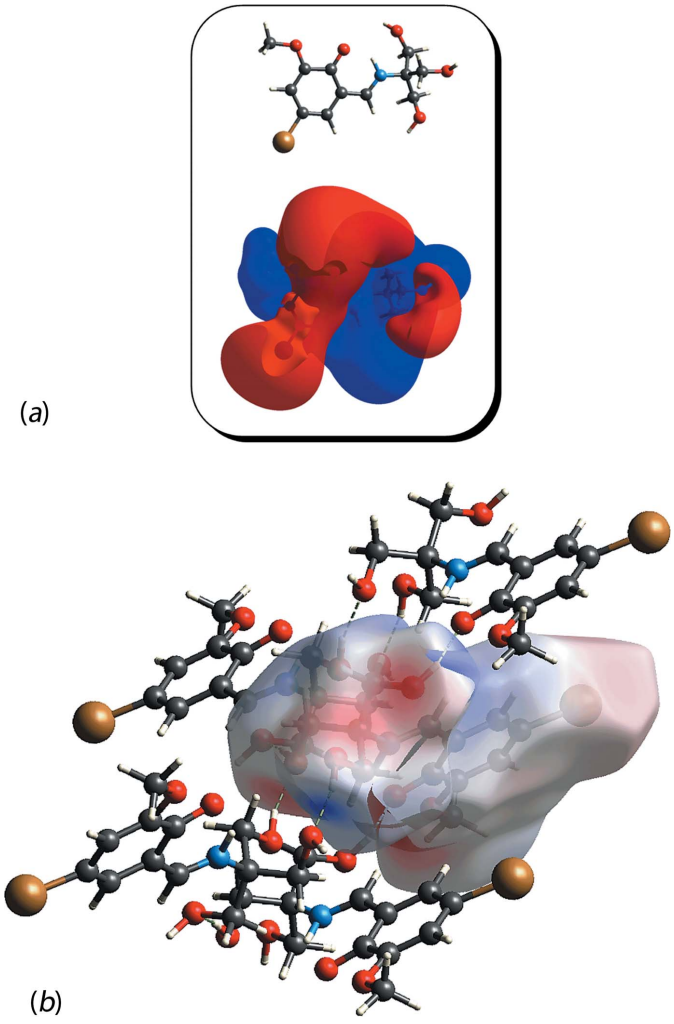

Figure 6
(*a*) The electrostatic potential map of (I) within the range of −0.008 to 0.008 au and (*b*) the ESP mapped over the Hirshfeld surface, showing the attraction between the electronegative (red) and electropositive (blue) sites in (I).

surface notwithstanding, as seen from Figs. 3(*c*) and 3(*d*), C···H and Br···H contacts are at distances greater than their respective van der Waals radii. Fig. 5 shows the O—H···O interactions formed between a reference molecule and symmetry-related molecules.

In order to gain a qualitative insight into the electrostatic interaction and rationalize the packing motif of the structure, the ESP was mapped over the Hirshfeld surface. The result illustrated in Fig. 6(*a*), shows that the electronegative sites are predominantly converged on O atoms and that, upon crystallization, the electronegative and electropositive sites are connected (Fig. 6*b*). It is noteworthy that despite bromine being an electrophilic element, it did not form a significant non-covalent interaction with neighbouring molecules in the inter-layer region where these atoms are directed. The closest contact in this region occurs with methyl-C···H12*C*^{i}, at 3.12 Å, *i.e* beyond the sum of the respective van der Waals radii (Spek, 2009) [symmetry code: (i) $x, -\frac{1}{2} - y, \frac{1}{2} + z$].

5. Database survey

There are several closely related structures to (I) in the crystallographic literature (Groom *et al.*, 2016). What might be termed the parent compound, *i.e*. with no substitution at the phenolate ring other than the imino group in the 2-position, (II), exists in the keto–amine tautomeric form and has been the subject of several investigations (Asgedom *et al.*, 1996; Tatar *et al.*, 2005). Similar zwitterionic structures are found in the 4-bromo, (III) (Martinez *et al.*, 2011), and 6-methoxy, (IV) (Odabaşoğlu *et al.*, 2003), derivatives, both closely related to (I), suggesting this is the most stable form for these molecules, at least in the solid state. Despite the similar electronic structures, conformational differences exist about the ring between (I) and (IV) as seen in the relative dispositions of the methoxy groups, *i.e*. C12—O5—C3—C2 is 177.7 (2)° in (I) but −165.75 (14)° in (IV) (Fig. 7). Differences in conformation of the methylhydroxy groups are also apparent, no doubt due to the different hydrogen-bonding patterns in the respective crystal structures.

6. Synthesis and crystallization

A solution of tris(hydroxymethyl)aminomethane (1.21 g, 0.01 mol) was added to an ethanolic solution of 5-bromo-3-methoxy-2-hydroxybenzaldehyde (2.31 g, 0.01 mol) and refluxed for 2 h. The solution was allowed to stand at room temperature, during which an orange solid formed. This was recrystallized by slow evaporation of its ethanol solution. Yield: 2.67 (80%). Yellow crystals. M.p. 465–466 K. Analysis calculated for $C_{12}H_{16}BrNO_5$: C 44.48, H 3.70, N 1.99%; found: C 44.81, H 3.42, N 1.64%. IR (cm^{-1}): 3330 (*b*) ν(N—H, O—

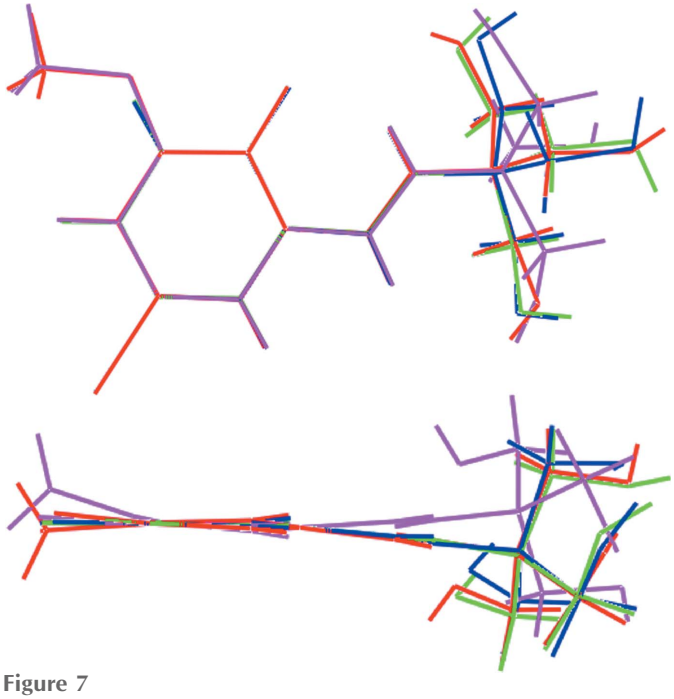

Figure 7
Overlay diagrams for (I) (red image), (II) (green), (III) (blue) and (IV) (pink). Images have been drawn so the benzene rings overlap.

Table 2
Experimental details.

Crystal data	
Chemical formula	$C_{12}H_{16}BrNO_5$
M_r	334.17
Crystal system, space group	Monoclinic, $P2_1/c$
Temperature (K)	293
a, b, c (Å)	12.2872 (9), 10.7186 (8), 10.5830 (8)
β (°)	108.462 (1)
V (Å^3)	1322.06 (17)
Z	4
Radiation type	Mo $K\alpha$
μ (mm^{-1})	3.13
Crystal size (mm)	0.26 × 0.10 × 0.08
Data collection	
Diffractometer	Bruker SMART APEX
Absorption correction	Multi-scan (*SADABS*; Sheldrick, 1996)
T_{min}, T_{max}	0.497, 0.788
No. of measured, independent and observed [$I > 2\sigma(I)$] reflections	5095, 2257, 1923
R_{int}	0.032
(sin $\theta/\lambda)_{max}$ (Å^{-1})	0.595
Refinement	
$R[F^2 > 2\sigma(F^2)]$, $wR(F^2)$, S	0.030, 0.068, 1.04
No. of reflections	2257
No. of parameters	185
No. of restraints	4
$\Delta\rho_{max}$, $\Delta\rho_{min}$ (e Å^{-3})	0.41, −0.54

Computer programs: *SMART* and *SAINT* (Bruker, 2008), *SHELXS97* (Sheldrick, 2008), *SHELXL2014* (Sheldrick, 2015), *ORTEP-3 for Windows* (Farrugia, 2012), *QMol* (Gans & Shalloway, 2001), *DIAMOND* (Brandenburg, 2006) and *publCIF* (Westrip, 2010).

H), 1640 (*s*) ν(C═N), 1528 (*m*) ν(−O−C═C−), 1066 (*m*) ν(C−O−C). ^{1}H NMR (400 MHz, $CDCl_3$): δ 8.35 [*s*, 1H, –N═C(H)], 7.01–7.10 (*m*, 1H, aryl H), 6.83–6.89 (*m*, 1H, aryl H), 5.06 (*s*, 3H, OH), 3.95 (*s*, 3H, OCH_3), 3.37–3.75 (*m*, 6H, aliphatic H).

7. Refinement

Crystal data, data collection and structure refinement details are summarized in Table 2. The carbon-bound H atoms were placed in calculated positions (C−H = 0.93–0.97 Å) and were included in the refinement in the riding-model approximation, with U_{iso}(H) set at 1.2–1.5U_{eq}(C). The O- and N-bound H atoms were located from difference Fourier maps and refined with distance restraints O−H = 0.82±0.01 Å and N−H = 0.86±0.01 Å, and with U_{iso}(H) set at 1.5U_{eq}(O) and U_{iso}(H) set at 1.2U_{eq}(N), respectively. Owing to poor agreement, several reflections, *i.e.* (−9 7 7), (−12 4 6), (−10 5 6) and (−3 3 2), were omitted from the final cycles of refinement.

Acknowledgements

The authors are grateful to Sunway University, the University of Malaya for financial assistance (grant No. RP017B-14AFR) and the Ministry of Higher Education of Malaysia (MOHE) Fundamental Research Grant Scheme (grant No. FP033-2014B) for supporting this research.

References

Asgedom, G., Sreedhara, A., Kivikoski, J., Valkonen, J., Kolehmainen, E. & Rao, C. P. (1996). *Inorg. Chem.* **35**, 5674–5683.
Back, D. F., Kopp, C. R., de Oliveira, G. M. & Piquini, P. C. (2012). *Polyhedron*, **36**, 21–29.
Brandenburg, K. (2006). *DIAMOND*. Crystal Impact GbR, Bonn, Germany.
Bruker (2008). *SMART* and *SAINT*. Bruker AXS Inc., Madison, Wisconsin, USA.
Chandrasekhar, V., Dey, A., Mota, A. J. & Colacio, E. (2013). *Inorg. Chem.* **52**, 4554–4561.
Das, C., Vaidya, S., Gupta, T., Frost, J. M., Righi, M., Brechin, E. K., Affronte, M., Rajaraman, G. & Shanmugam, M. (2015). *Chem. Eur. J.* **21**, 15639–15650.
Dey, S. K., Mitra, P. & Mukherjee, A. (2015). *Cryst. Growth Des.* **15**, 706–717.
Dey, S. K. & Mukherjee, A. (2014). *New J. Chem.* **38**, 4985–4995.
Farrugia, L. J. (2012). *J. Appl. Cryst.* **45**, 849–854.
Gans, J. & Shalloway, D. (2001). *J. Mol. Graph. Model.* **19**, 557–559.
Groom, C. R., Bruno, I. J., Lightfoot, M. P. & Ward, S. C. (2016). *Acta Cryst.* B**72**, 171–179.
Halevas, E., Tsave, O., Yavropoulou, M. P., Hatzidimitriou, A., Yovos, J. G., Psycharis, V., Gabriel, C. & Salifoglou, A. (2015). *J. Inorg. Biochem.* **147**, 99–115.
Lee, S. M., Sim, K. S. & Lo, K. M. (2015). *Inorg. Chim. Acta*, **429**, 195–208.
Martinez, R. F., Ávalos, M., Babiano, R., Cintas, P., Jiménez, J. L., Light, M. E. & Palacios, J. C. (2011). *Eur. J. Org. Chem.* pp. 3137–3145.
McKinnon, J. J., Jayatilaka, D. & Spackman, M. A. (2007). *Chem Commun.* pp. 3814–3816.
Odabaşoğlu, M., Albayrak, Ç., Büyükgüngör, O. & Lönnecke, P. (2003). *Acta Cryst.* C**59**, o616–o619.
Rehder, D., Pessoa, J. C., Geraldes, C. F. G. C., Castro, M. M. C. A., Kabanos, T., Kiss, T., Meier, B., Micera, G., Pettersson, L., Rangel, M., Salifoglou, A., Turel, I. & Wang, D. (2002). *J. Biol. Inorg. Chem.* **7**, 384–396.
Sheldrick, G. M. (1996). *SADABS*. University of Göttingen, Germany.
Sheldrick, G. M. (2008). *Acta Cryst.* A**64**, 112–122.
Sheldrick, G. M. (2015). *Acta Cryst.* C**71**, 3–8.
Spackman, M. A. & Jayatilaka, D. (2009). *CrystEngComm*, **11**, 19–32.
Spackman, M. A. & McKinnon, J. J. (2002). *CrystEngComm*, **4**, 378–392.
Spackman, M. A., McKinnon, J. J. & Jayatilaka, D. (2008). *CrystEngComm*, **10**, 377–388.
Spek, A. L. (2009). *Acta Cryst.* D**65**, 148–155.
Tatar, L., Nazir, H., Gümüşer, M., Kale, C. & Atakol, O. (2005). *Z. Kristallogr.* **220**, 639–642.
Tsave, O., Halevas, E., Yavropoulou, M. P., Kosmidis Papadimitriou, A., Yovos, J. G., Hatzidimitriou, A., Gabriel, C., Psycharis, V. & Salifoglou, A. (2015). *J. Inorg. Biochem.* **152**, 123-137.
Westrip, S. P. (2010). *J. Appl. Cryst.* **43**, 920–925.
Wolff, S. K., Grimwood, D. J., McKinnon, J. J., Turner, M. J., Jayatilaka, D. & Spackman, M. A. (2012). *Crystal Explorer*. The University of Western Australia.
Wu, G., Hewitt, I. J., Mameri, S., Lan, Y., Clérac, R., Anson, C. E., Qiu, S. & Powell, A. K. (2007). *Inorg. Chem.* **46**, 7229–7231.
Zou, H.-H., Sheng, L.-B., Liang, F. P., Chen, Z.-L. & Zhang, Y.-Q. (2015). *Dalton Trans.* **44**, 18544–18552.

supporting information

Acta Cryst. (2016). E**72**, 1223-1227 [https://doi.org/10.1107/S2056989016012159]

Zwitterionic 4-bromo-6-methoxy-2-{[tris(hydroxymethyl)methyl]iminiumylmethyl}phenolate: crystal structure and Hirshfeld surface analysis

See Mun Lee, Kong Mun Lo, Sang Loon Tan and Edward R. T. Tiekink

Computing details

Data collection: *SMART* (Bruker, 2008); cell refinement: *SMART* (Bruker, 2008); data reduction: *SAINT* (Bruker, 2008); program(s) used to solve structure: *SHELXS97* (Sheldrick, 2008); program(s) used to refine structure: *SHELXL2014* (Sheldrick, 2015); molecular graphics: *ORTEP-3 for Windows* (Farrugia, 2012), *QMol* (Gans & Shalloway, 2001), *DIAMOND* (Brandenburg, 2006); software used to prepare material for publication: *publCIF* (Westrip, 2010).

4-Bromo-2-((1*E*)-{[1,3-dihydroxy-2-(hydroxymethyl)propan-2-yl]iminiumyl}methyl)-6-methoxybenzen-1-olate

Crystal data

$C_{12}H_{16}BrNO_5$
M_r = 334.17
Monoclinic, $P2_1/c$
a = 12.2872 (9) Å
b = 10.7186 (8) Å
c = 10.5830 (8) Å
β = 108.462 (1)°
V = 1322.06 (17) Å^3
Z = 4
$F(000)$ = 680
D_x = 1.679 Mg m^{-3}
Mo $K\alpha$ radiation, λ = 0.71073 Å
Cell parameters from 1493 reflections
θ = 2.6–27.9°
μ = 3.13 mm^{-1}
T = 293 K
Prism, yellow
0.26 × 0.10 × 0.08 mm

Data collection

Bruker SMART APEX diffractometer
Radiation source: fine-focus sealed tube
Graphite monochromator
φ and ω scans
Absorption correction: multi-scan (SADABS; Sheldrick, 1996)
T_{min} = 0.497, T_{max} = 0.788
5095 measured reflections
2257 independent reflections
1923 reflections with $I > 2\sigma(I)$
R_{int} = 0.032
θ_{max} = 25.0°, θ_{min} = 1.8°
h = −10→14
k = −12→12
l = −9→12

Refinement

Refinement on F^2
Least-squares matrix: full
$R[F^2 > 2\sigma(F^2)]$ = 0.030
$wR(F^2)$ = 0.068
S = 1.04
2257 reflections
185 parameters
4 restraints
Hydrogen site location: mixed
$w = 1/[\sigma^2(F_o^2) + (0.0206P)^2 + 0.8903P]$ where $P = (F_o^2 + 2F_c^2)/3$
$(\Delta/\sigma)_{max} < 0.001$
$\Delta\rho_{max}$ = 0.41 e Å^{-3}
$\Delta\rho_{min}$ = −0.54 e Å^{-3}

Special details

Geometry. All esds (except the esd in the dihedral angle between two l.s. planes) are estimated using the full covariance matrix. The cell esds are taken into account individually in the estimation of esds in distances, angles and torsion angles; correlations between esds in cell parameters are only used when they are defined by crystal symmetry. An approximate (isotropic) treatment of cell esds is used for estimating esds involving l.s. planes.

Fractional atomic coordinates and isotropic or equivalent isotropic displacement parameters (Å²)

	x	*y*	*z*	U_{iso}*/U_{eq}
Br1	0.45516 (2)	−0.01276 (3)	0.80991 (3)	0.01835 (11)
O1	0.79706 (16)	0.09687 (18)	0.52558 (18)	0.0134 (4)
O2	1.05037 (18)	0.27428 (18)	0.60436 (19)	0.0141 (5)
H2O	1.083 (2)	0.2087 (17)	0.632 (3)	0.021*
O3	0.96322 (18)	0.60240 (19)	0.62300 (19)	0.0174 (5)
H3O	0.948 (3)	0.641 (3)	0.5535 (19)	0.026*
O4	0.85256 (17)	0.54263 (18)	0.83553 (19)	0.0132 (4)
H4O	0.824 (3)	0.517 (3)	0.891 (2)	0.020*
O5	0.70096 (17)	−0.12504 (18)	0.49502 (19)	0.0153 (5)
N1	0.8572 (2)	0.2954 (2)	0.6738 (2)	0.0118 (5)
H1N	0.865 (3)	0.245 (2)	0.615 (2)	0.014*
C1	0.7122 (2)	0.1554 (3)	0.6915 (3)	0.0125 (6)
C2	0.7298 (2)	0.0719 (3)	0.5940 (3)	0.0110 (6)
C3	0.6701 (2)	−0.0452 (3)	0.5783 (3)	0.0122 (6)
C4	0.5921 (2)	−0.0711 (3)	0.6427 (3)	0.0133 (6)
H4	0.5531	−0.1467	0.6289	0.016*
C5	0.5715 (2)	0.0190 (3)	0.7308 (3)	0.0146 (6)
C6	0.6309 (2)	0.1276 (3)	0.7580 (3)	0.0140 (6)
H6	0.6186	0.1835	0.8193	0.017*
C7	0.7801 (2)	0.2645 (3)	0.7279 (3)	0.0109 (6)
H7	0.7689	0.3161	0.7933	0.013*
C8	0.9361 (2)	0.4026 (3)	0.7066 (3)	0.0110 (6)
C9	1.0558 (2)	0.3539 (3)	0.7151 (3)	0.0129 (6)
H9A	1.1060	0.4239	0.7159	0.016*
H9B	1.0878	0.3079	0.7975	0.016*
C10	0.8904 (2)	0.4963 (2)	0.5932 (3)	0.0120 (6)
H10A	0.8904	0.4597	0.5094	0.014*
H10B	0.8124	0.5201	0.5856	0.014*
C11	0.9462 (2)	0.4610 (3)	0.8413 (3)	0.0121 (6)
H11A	0.9492	0.3952	0.9052	0.014*
H11B	1.0175	0.5076	0.8725	0.014*
C12	0.6500 (3)	−0.2459 (3)	0.4763 (3)	0.0216 (7)
H12A	0.6684	−0.2879	0.5606	0.032*
H12B	0.6791	−0.2933	0.4170	0.032*
H12C	0.5683	−0.2380	0.4388	0.032*

Atomic displacement parameters (Å²)

	U^{11}	U^{22}	U^{33}	U^{12}	U^{13}	U^{23}
Br1	0.01640 (17)	0.01891 (18)	0.02421 (18)	−0.00122 (13)	0.01279 (13)	0.00285 (13)
O1	0.0139 (11)	0.0159 (11)	0.0136 (10)	−0.0018 (8)	0.0089 (9)	−0.0016 (8)
O2	0.0205 (12)	0.0093 (10)	0.0139 (11)	0.0039 (9)	0.0075 (9)	0.0016 (8)
O3	0.0284 (13)	0.0112 (11)	0.0141 (11)	−0.0034 (9)	0.0091 (10)	0.0029 (8)
O4	0.0141 (11)	0.0153 (11)	0.0145 (11)	0.0004 (8)	0.0108 (9)	−0.0009 (9)
O5	0.0192 (12)	0.0123 (10)	0.0173 (11)	−0.0026 (9)	0.0099 (9)	−0.0049 (9)
N1	0.0151 (13)	0.0091 (12)	0.0109 (13)	−0.0001 (10)	0.0034 (11)	−0.0023 (10)
C1	0.0106 (15)	0.0127 (15)	0.0145 (15)	−0.0002 (12)	0.0043 (12)	0.0015 (12)
C2	0.0079 (14)	0.0123 (15)	0.0110 (14)	0.0025 (11)	0.0008 (12)	0.0037 (12)
C3	0.0094 (15)	0.0149 (15)	0.0126 (15)	0.0007 (12)	0.0038 (12)	−0.0008 (12)
C4	0.0132 (16)	0.0104 (14)	0.0142 (15)	−0.0009 (12)	0.0013 (12)	0.0009 (12)
C5	0.0122 (15)	0.0180 (16)	0.0147 (15)	−0.0013 (12)	0.0060 (12)	0.0054 (12)
C6	0.0140 (15)	0.0140 (15)	0.0145 (15)	0.0035 (12)	0.0052 (12)	0.0007 (12)
C7	0.0121 (15)	0.0098 (14)	0.0115 (14)	0.0028 (11)	0.0049 (12)	0.0025 (11)
C8	0.0124 (15)	0.0105 (14)	0.0114 (14)	−0.0008 (11)	0.0055 (12)	−0.0004 (11)
C9	0.0137 (16)	0.0124 (15)	0.0137 (15)	−0.0019 (12)	0.0056 (12)	−0.0010 (11)
C10	0.0132 (14)	0.0117 (14)	0.0118 (14)	0.0021 (12)	0.0052 (11)	−0.0028 (12)
C11	0.0123 (15)	0.0117 (14)	0.0128 (15)	0.0016 (12)	0.0048 (12)	−0.0002 (11)
C12	0.0263 (19)	0.0138 (16)	0.0267 (18)	−0.0091 (13)	0.0112 (15)	−0.0070 (13)

Geometric parameters (Å, º)

Br1—C5	1.902 (3)	C4—C5	1.420 (4)
O1—C2	1.287 (3)	C4—H4	0.9300
O2—C9	1.434 (3)	C5—C6	1.355 (4)
O2—H2O	0.818 (10)	C6—H6	0.9300
O3—C10	1.419 (3)	C7—H7	0.9300
O3—H3O	0.815 (10)	C8—C11	1.525 (4)
O4—C11	1.432 (3)	C8—C10	1.529 (4)
O4—H4O	0.819 (10)	C8—C9	1.536 (4)
O5—C3	1.365 (3)	C9—H9A	0.9700
O5—C12	1.425 (3)	C9—H9B	0.9700
N1—C7	1.295 (4)	C10—H10A	0.9700
N1—C8	1.473 (4)	C10—H10B	0.9700
N1—H1N	0.856 (10)	C11—H11A	0.9700
C1—C7	1.417 (4)	C11—H11B	0.9700
C1—C6	1.424 (4)	C12—H12A	0.9600
C1—C2	1.432 (4)	C12—H12B	0.9600
C2—C3	1.438 (4)	C12—H12C	0.9600
C3—C4	1.369 (4)		
C9—O2—H2O	109 (2)	N1—C8—C10	106.1 (2)
C10—O3—H3O	105 (2)	C11—C8—C10	111.4 (2)
C11—O4—H4O	107 (2)	N1—C8—C9	107.2 (2)
C3—O5—C12	117.3 (2)	C11—C8—C9	107.0 (2)

C7—N1—C8	127.9 (2)	C10—C8—C9	112.1 (2)
C7—N1—H1N	115 (2)	O2—C9—C8	111.0 (2)
C8—N1—H1N	117 (2)	O2—C9—H9A	109.4
C7—C1—C6	118.9 (3)	C8—C9—H9A	109.4
C7—C1—C2	120.1 (3)	O2—C9—H9B	109.4
C6—C1—C2	121.0 (3)	C8—C9—H9B	109.4
O1—C2—C1	123.0 (3)	H9A—C9—H9B	108.0
O1—C2—C3	120.8 (3)	O3—C10—C8	107.6 (2)
C1—C2—C3	116.2 (3)	O3—C10—H10A	110.2
O5—C3—C4	125.2 (3)	C8—C10—H10A	110.2
O5—C3—C2	112.7 (2)	O3—C10—H10B	110.2
C4—C3—C2	122.1 (3)	C8—C10—H10B	110.2
C3—C4—C5	119.2 (3)	H10A—C10—H10B	108.5
C3—C4—H4	120.4	O4—C11—C8	112.6 (2)
C5—C4—H4	120.4	O4—C11—H11A	109.1
C6—C5—C4	121.8 (3)	C8—C11—H11A	109.1
C6—C5—Br1	119.3 (2)	O4—C11—H11B	109.1
C4—C5—Br1	118.8 (2)	C8—C11—H11B	109.1
C5—C6—C1	119.3 (3)	H11A—C11—H11B	107.8
C5—C6—H6	120.3	O5—C12—H12A	109.5
C1—C6—H6	120.3	O5—C12—H12B	109.5
N1—C7—C1	122.7 (3)	H12A—C12—H12B	109.5
N1—C7—H7	118.6	O5—C12—H12C	109.5
C1—C7—H7	118.6	H12A—C12—H12C	109.5
N1—C8—C11	113.2 (2)	H12B—C12—H12C	109.5

C7—C1—C2—O1	−7.6 (4)	C2—C1—C6—C5	1.7 (4)
C6—C1—C2—O1	175.5 (2)	C8—N1—C7—C1	−177.2 (3)
C7—C1—C2—C3	170.7 (2)	C6—C1—C7—N1	178.9 (3)
C6—C1—C2—C3	−6.2 (4)	C2—C1—C7—N1	1.9 (4)
C12—O5—C3—C4	−1.6 (4)	C7—N1—C8—C11	16.6 (4)
C12—O5—C3—C2	177.7 (2)	C7—N1—C8—C10	−105.8 (3)
O1—C2—C3—O5	5.3 (4)	C7—N1—C8—C9	134.3 (3)
C1—C2—C3—O5	−173.1 (2)	N1—C8—C9—O2	45.9 (3)
O1—C2—C3—C4	−175.4 (3)	C11—C8—C9—O2	167.6 (2)
C1—C2—C3—C4	6.2 (4)	C10—C8—C9—O2	−70.0 (3)
O5—C3—C4—C5	177.5 (3)	N1—C8—C10—O3	178.8 (2)
C2—C3—C4—C5	−1.8 (4)	C11—C8—C10—O3	55.2 (3)
C3—C4—C5—C6	−3.2 (4)	C9—C8—C10—O3	−64.6 (3)
C3—C4—C5—Br1	175.5 (2)	N1—C8—C11—O4	−80.2 (3)
C4—C5—C6—C1	3.2 (4)	C10—C8—C11—O4	39.2 (3)
Br1—C5—C6—C1	−175.5 (2)	C9—C8—C11—O4	162.0 (2)
C7—C1—C6—C5	−175.2 (3)		

Hydrogen-bond geometry (Å, º)

D—H···*A*	*D*—H	H···*A*	*D*···*A*	*D*—H···*A*
N1—H1*N*···O1	0.85 (2)	1.90 (2)	2.608 (3)	140 (3)

O2—H2*O*···O4^{i}	0.82 (2)	1.93 (2)	2.741 (3)	170 (3)
O3—H3*O*···O2^{ii}	0.81 (2)	1.91 (2)	2.704 (3)	167 (4)
O4—H4*O*···O1^{iii}	0.82 (3)	1.98 (3)	2.760 (3)	158 (3)
C7—H7···O1^{iii}	0.93	2.55	3.429 (4)	158
C9—H9*B*···O3^{i}	0.97	2.51	3.242 (4)	132
C11—H11*B*···O1^{iv}	0.97	2.39	3.353 (3)	171

Symmetry codes: (i) −*x*+2, *y*−1/2, −*z*+3/2; (ii) −*x*+2, −*y*+1, −*z*+1; (iii) *x*, −*y*+1/2, *z*+1/2; (iv) −*x*+2, *y*+1/2, −*z*+3/2.